

Radiation tolerant semiconductor sensors for tracking detectors

Michael Moll*

CERN, PH Department, 1211 Geneva 23, Switzerland

On behalf of the RD50 Collaboration¹

Available online 24 May 2006

Abstract

The CERN RD50 collaboration “Development of Radiation Hard Semiconductor Devices for Very High Luminosity Colliders” is developing radiation tolerant tracking detectors for the upgrade of the Large Hadron Collider at CERN (Super-LHC). One of the main challenges arising from the target luminosity of $10^{35} \text{ cm}^{-2} \text{ s}^{-1}$ are the unprecedented high radiation levels. Over the anticipated 5 years lifetime of the experiment a cumulated fast hadron fluence of about 10^{16} cm^{-2} will be reached for the innermost tracking layers. Further challenges are the expected reduced bunch crossing time of about 10 ns and the high track density calling for fast and high granularity detectors which also fulfill the boundary conditions of low radiation length and low costs. After a short description of the expected radiation damage after a fast hadron fluence of 10^{16} cm^{-2} , several R&D approaches aiming for radiation tolerant sensor materials (defect and material engineering) and sensor designs (device engineering) are reviewed and discussed. Special emphasis is put on detectors based on oxygen-enriched Floating Zone (FZ) silicon, Czochralski (CZ) silicon and epitaxial silicon. Furthermore, recent advancements on SiC and GaN detectors, single type column 3D detectors and p-type detectors will be presented.

© 2006 Elsevier B.V. All rights reserved.

PACS: 92.40.Gx; 29.40.Wk; 61.82.Fk

Keywords: Radiation damage; Semiconductor detectors; Silicon particle detectors; Defect engineering; SLHC

1. Introduction

The Large Hadron Collider (LHC) at CERN is expected to deliver first proton–proton collisions before the end of 2007. At the end of the following commissioning phase the design luminosity of $10^{34} \text{ cm}^{-2} \text{ s}^{-1}$ at proton energies of 7 TeV shall be reached for the two multipurpose experiments ATLAS and CMS. The exposure of all detector components to high radiation levels arising from the high luminosity operation has been well anticipated. A long R&D phase preceding the construction of the detector components gives presently confidence that the detectors will survive an integrated luminosity of 500 fb^{-1} , corresponding to a 10-year operation of the LHC. However, it is obvious that the main part of the presently used detectors

would not survive or would not be operational for the proposed upgrade of the machine to a 10 times higher luminosity (Super-LHC or SLHC) with a proposed accumulated luminosity of 2500 fb^{-1} [1,2]. A dedicated R&D program is therefore urgently needed and partly already under way to develop new detector technologies for the innermost tracking layers and replacements for most of the outer detector components.

Fig. 1 gives an indication about the cumulated hadron fluences after an integrated luminosity of 2500 fb^{-1} . For the innermost tracking layers fluences of more than $1 \times 10^{16} \text{ cm}^{-2}$ are expected. Besides these unprecedented high radiation levels the increase in the track density and the proposed reduction of the bunch crossing time from 25 ns to about 10 ns will pose the most severe challenges. Faster detectors with finer granularity are therefore needed. This means for example that the pixel detectors will have to cover the tracking volume to higher radii (see shaded areas in Fig. 1) pushing the microstrip detector

*Tel.: +41 22 767 2495; fax: +41 22 767 69629.

E-mail address: michael.moll@cern.ch

¹A complete author list can be found at: <http://cern.ch/rd50/>.

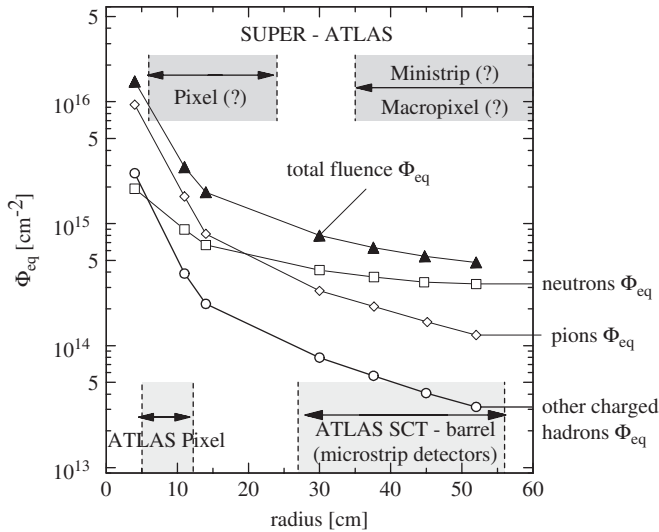


Fig. 1. Hadron fluences expected in the inner SUPER-ATLAS detector after 5 years (2500 fb⁻¹). The data have been taken from a calculation for the ATLAS detector [3] and are scaled to the expected SUPER-ATLAS integrated luminosity. While the exact SUPER-ATLAS geometry is not yet known, the presented data can be used as a rough estimate.

system further outside. The microstrip detectors themselves will have to be reduced in strip size making the difference between microstrip and pixel detectors less and less distinct as, e.g. expressed in the naming of some newly developed devices as “macropixel” or “ministrips”. In any case the increased granularity will call for more cost effective technologies than presently existing since otherwise a detector upgrade could not be afforded.

The RD50 collaboration “Development of Radiation Hard Semiconductor Devices for Very High Luminosity Colliders” [4] was formed in 2002 with the aim to develop semiconductor sensors matching the above mentioned SLHC requirements. These efforts are now closely linked to the increasing upgrade activities of ATLAS and CMS which are expressed by the increasing frequency of their upgrade workshops [5,6].

Only some specific topics of the RD50 scientific program will be described. More detailed information can be found in Refs. [4,7], in recent conference proceedings [8–11] and in literature cited there.

2. Radiation damage and strategies to cope with it

2.1. Radiation damage

The radiation damage to silicon sensors can be divided into two general types of damage. The first is caused by Ionizing Energy Loss (IEL) and produces surface damage. Positive charge is accumulated in the oxide (SiO₂) and interface states at the Si/SiO₂ interface are created as a consequence. This can influence the detector capacitance, rise the noise and might have a negative impact on the breakdown behavior. The second type of damage is arising from Non-Ionizing Energy Loss (NIEL) which is causing

the creation of crystal defects in the silicon bulk. It is this type of damage which is presently the main concern and which expresses itself in the following three detector deterioration effects:

- A change of the effective doping concentration with severe consequences for the electric field profile and the operating voltage needed for full depletion.
- A fluence proportional increase of the leakage current, increasing the electronic noise and the power consumption and dissipation.
- An increase of the charge carrier trapping leading to a reduction of the effective drift length both for electrons and holes and thus to a reduction of the charge collection efficiency (CCE) of the detector.

Since there are only very little experimental data regarding the impact of an irradiation to a fluence of 10¹⁶ cm⁻² quantitative values can only be extrapolated from experiments performed at lower fluences. Assuming an annealing of 14 days at room temperature after exposure to a 1 MeV neutron equivalent charged hadrons fluence of 10¹⁶ cm⁻² the following can be extrapolated. The leakage current density rises to a level of ≈400 mA/cm² (20 °C) or ≈25 mA/cm² (–10 °C) [12] rendering cooling of the detectors inevitable to reduce noise and power consumption. The effective trapping times for holes and electrons is reduced to less than 200 ps corresponding to a drift length of about 30 μm for electrons and only 7 μm for holes [13,14]. The difference between hole and electron drift length is thereby mainly arising from the three times higher drift velocity of the electrons.

While for the leakage current and the trapping no strong variations between different (defect engineered) silicon materials have been observed, the change of the effective doping concentration is strongly influenced by the choice of the silicon material (see Section 3). In standard n-type FZ silicon the net space charge changes from positive to negative due to the radiation-induced generation of deep acceptors. Accordingly, it is expected that the depletion of a type inverted p⁺–n detector starts from the n⁺-contact. Following this assumption and taking, e.g. the data given in Ref. [15] for FZ silicon the depletion depth would be reduced to about 50 μm for a detector operating at 500 V. This number must be taken with care however. On the one hand, the increase of the effective space charge depends strongly on the used silicon material and on the other hand the formation of the electric field is not as simple as stated above. A so-called “double-junction” is appearing after irradiation with high fluences [16,17] being formed by electric fields growing from the front and the back contact. This makes further experimental and simulation work necessary to understand the electric field distribution and its impact on the CCE in highly irradiated devices.

Each of the above-mentioned effects is changing in time at room temperature (annealing). While the leakage current and the electron trapping are annealing in a beneficial way,

the hole trapping is further increased [18]. The effective doping concentration is “reverse annealing” meaning that negative space charge is built up. This is a detrimental effect in standard FZ silicon, but can, as will be shown later for Czochralski (CZ) and Epitaxial Silicon (EPI), also be a beneficial one.

Finally the combination of trapping and incomplete depletion leads to a strong deterioration of the CCE and consequently the signal-to-noise ratio, for both, pixel and strip detectors.

Only a very brief overview about the macroscopic radiation effects was given here. A detailed description or a review about the underlying microscopic defects is beyond the scope of this article and can be found elsewhere (e.g. Refs. [3,19–23]).

2.2. Development of radiation tolerant detectors

Each of the above-mentioned effects influences the signal-to-noise ratio of a detector which is, in the end, the quantity deciding on the tracking capabilities of an irradiated device. The extent to which a detector suffers from the radiation depends however not only on the above-mentioned radiation effects, the operation bias and temperature and the irradiation and annealing history, but also on the geometry and working principle of the device. This makes it impossible to give, e.g. a global figure of the CCE after irradiation for different types of detectors with different types of read-out electronics. It is thus very reasonable to investigate the impact of radiation on the detector bulk properties separately from the influence of the detector geometry on the radiation tolerance and then combine the most radiation tolerant material with the most radiation tolerant geometry.

In the following the most recent results of the RD50 collaboration regarding the “Material Engineering” (Section 3) and “Device Engineering” (Section 4) approaches to obtain more radiation tolerant detectors are presented. It should however be mentioned that the “Change of detector operational conditions” also might lead to more radiation tolerant detectors. This approach is presently followed by the RD39 project “Cryogenic Tracking Detectors” [24].

3. Material engineering

3.1. Material engineering—overview

There are various semiconductors that could be used as tracking detector bulk material. Among those n-type Floating Zone (FZ) silicon is the most prominent and mostly used. Several approaches have been undertaken to “defect engineer” FZ silicon in order to make it more radiation tolerant. FZ silicon has been enriched with oxygen by putting an oxygen jet on the melting zone of a FZ ingot and by diffusing oxygen into silicon wafers by high temperature long-term treatments (DOFZ—Diffusion

Oxygenated FZ silicon) [19]. FZ silicon was furthermore enriched with Nitrogen, Carbon, Germanium and Tin to test the impact on the radiation tolerance [25]. There are ongoing experiments to understand the impact of “pre-irradiation”, where a silicon wafer is irradiated in a nuclear reactor prior to be processed into a detector [26]. There have been experiments to increase the oxygen dimer (O_2) concentration in FZ silicon by electron irradiation [27]. Furthermore, detectors are exposed to hydrogen plasma in order to increase the hydrogen content of the detector [28].

Many of these experiments have been concluded with negative results while some are still ongoing and a few, like the oxygen enrichment, gave already positive results. They all have in common, with the exception of the DOFZ technique, that they are quite complicate to apply. Only recently the different growth techniques of silicon came back into focus as source for different materials. In Sections 3.2 and 3.3 it will be shown that CZ and EPI offer an improved radiation tolerance with respect to FZ silicon.

A more drastic “material engineering” approach is the replacement of silicon by another semiconductor. Table 1 summarizes some relevant properties of potential tracking detector materials. Germanium might be excluded due to its small band gap which makes operation close to room temperature impossible. GaAs was identified to be very sensitive to charged hadron irradiation [38]. Diamond is, although still very expensive, a promising tracking detector material candidate [29,30]. It will be used for beam condition monitoring systems of the ATLAS and CMS experiment in areas with high radiation levels. Also hydrogenated amorphous Silicon deposited directly on readout chips is under investigation [31]. The RD50 collaboration is focusing on SiC and GaN which will be discussed in Section 3.4. A more detailed review regarding non-silicon tracking detector materials can be found in Ref. [32].

3.2. Czochralski silicon and Magnetic Czochralski (MCZ)

CZ and MCZ have, due to their specific growth technique, much higher oxygen content than Float Zone (FZ) and even Diffusion Oxygenated FZ (DOFZ) silicon. This is demonstrated in Fig. 2 showing the oxygen depth profile of CZ and DOFZ silicon [3] as measured with a special Secondary Ion Mass Spectroscopy (SIMS) technology [42].

CZ silicon detectors have meanwhile been successfully processed at CiS (Germany), Helsinki University of Technology (Finland), CNM (Spain), IRST (Italy) and BNL (USA). Several irradiation experiments have been performed with reactor neutrons [43], high energy (23 GeV [14,44]) and low energy (10, 20, and 30 MeV [45]) protons, 190 MeV pions [46], 900 MeV electrons [47] and Co^{60} gammas [43] revealing clear advantages of MCZ and especially CZ silicon against FZ and DOFZ silicon.

Table 1

Properties of some semiconductor materials that could be used as tracking detector bulk material [32–41]

Property	Si	Diamond	Ge	4H-SiC	GaAs	GaN	a-Si (H)
Z	14	6	32	14/6	31/33	31/7	14
Density (g/cm ³)	2.33	3.52	5.32	3.22	5.32	6.2	~2.3
Dielectric constant	11.9	5.7	16.2	9.7	12.4	8.9	—
E_g (eV)	1.12	5.48	0.66	3.27	1.42	3.39	1.7
μ_e (cm ² /V s)	1450	1800	3900	450	9200	1000	1–10
μ_h (cm ² /V s)	505	1200–1600	1800	115	320	30	0.005–0.01
Displacement (eV)	13–25	43	28	20–35	10	~10–20	—
e–h energy (eV)	3.63	13.1	2.96	8.4	4.35	8.9	~4.8
e–h pairs/ μ m	107	47	247	51	130	~90	~37
Radiation length, X_0 (cm)	9.36	12.15	2.30	8.7	2.3	2.7	—
e–h pairs/ X_0 (10 ⁶ cm ^{−1})	10.0	5.7	5.67	4.5	2.99	~2–3	—

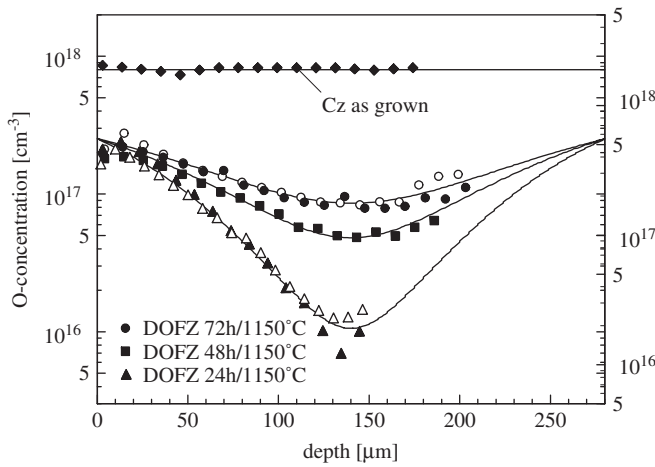


Fig. 2. Oxygen depth profiles for CZ and three different types of DOFZ silicon as measured by SIMS [3].

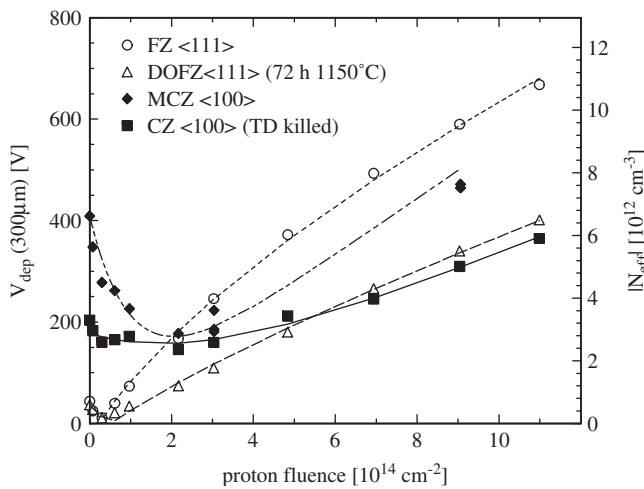


Fig. 3. Comparison of standard FZ and oxygenated DOFZ Float Zone silicon with Czochralski (CZ) and Magnetic Czochralski (MCZ) silicon detectors in a CERN irradiation scenario (after each irradiation step the devices are annealed for 4 min at 80 °C and then measured. The result is plotted against the cumulated fluence) with 23 GeV protons [46].

Fig. 3 shows a comparison of the radiation-induced change of the depletion voltage for different silicon materials during a 23 GeV proton irradiation [46]. Com-

paring the results for FZ and DOFZ detectors a strongly reduced depletion voltage is observed for the oxygen enriched material. The use of CZ silicon does not seem to improve the radiation tolerance further and the lower resistivity MCZ silicon even inhibits a higher depletion voltage than DOFZ silicon at all fluences. The only visible amelioration is that the overall variation of the depletion voltage during irradiation is less in the CZ materials giving more stable conditions during detector operation. The huge advantage of the n-type CZ and MCZ is only displayed in more subtle experiments that probe the electric field inside the irradiated devices and measure the signal (charge) delivered by the device. With Transient Charge Technique (TCT) measurements it has been shown that both materials do not undergo type inversion (the sign of the total space charge remains positive) while the effective trapping times are very similar to the ones of standard and DOFZ silicon [14]. These results have now to be further confirmed and complemented by more detailed CCE measurements in simple and segmented devices in order to understand the role of the double junction effect on CZ silicon. CZ silicon might well become the ideal detector material for low cost single sided radiation tolerant p-in-n detectors.² The high electric field will stay on the structured side of the device even after high fluences. Furthermore, the reverse annealing could even be used as a beneficial effect as will be demonstrated for the also not type inverting EPI in the following section.

3.3. Epitaxial silicon

Oxygen depth profiles for EPI layers of different thickness are shown in Fig. 4 [48]. It can be seen that oxygen from the low resistivity CZ substrate layer diffused into the epitaxial layer during the epitaxial growth process.

It is very interesting that the average oxygen content, at least for the thicker epi-layers (e.g. 50 μ m: $\langle [O] \rangle = 9 \times 10^{16} \text{ cm}^{-3}$), is lower than the average oxygen content in some of the DOFZ silicon materials (e.g. 72 h DOFZ:

²For a comparison between p-in-n technology and n-in-p or n-in-n technology see Section 4.

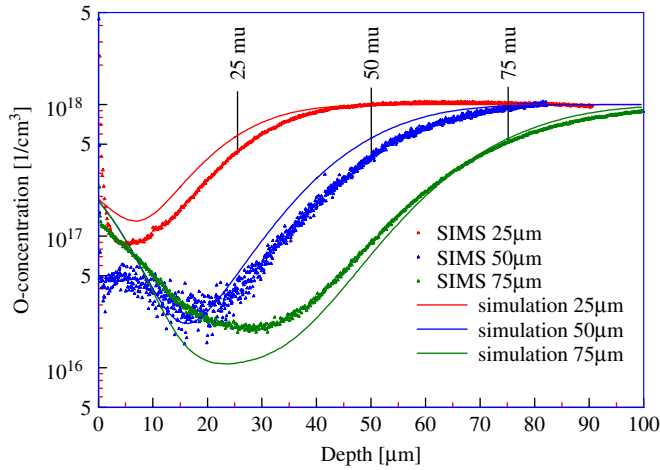


Fig. 4. Oxygen depth profiles measured by SIMS for detectors with three different epi-layer thicknesses (25, 50 and 75 μm) [48].

$1.2 \times 10^{17} \text{ cm}^{-3}$, see Fig. 2). This is a clear hint that the improved radiation tolerance of EPI is not only related to the oxygen content but is also linked to other aspects of the material. A very likely cause is oxygen dimers (O_2) that are diffusing from the CZ substrate into the epi-layer during the processing of the epi-layer. These neutral impurities are then transformed by radiation into shallow donors [49].

Detectors have been produced from epitaxial layers in various facilities and irradiation experiments have been performed with 23 GeV protons [48–52], MeV neutrons [48,50,52], 900 MeV electrons [47] and 58 MeV Lithium ions [53]. An example for the radiation-induced change of the effective doping concentration with 23 GeV proton fluence is shown in Fig. 5.

As for the CZ material the increase of the effective doping concentration N_{eff} for large fluences has been proven to be a built up of positive space charge. The detectors are thus not type inverted. The increase of N_{eff} is depending on the layer thickness. While a strong increase for 25 μm layers is observed, the depletion voltage for the 75 μm layers does hardly change up to the highest fluence. This is obviously related to the oxygen profiles shown in Fig. 4. However, as stated above, not the oxygen itself but rather the oxygen dimer concentration is assumed to be the reason for the observed differences.

A CCE measurement performed with a ^{90}Sr -source on 23 GeV proton and MeV neutron irradiated epitaxial detectors is shown in Fig. 6 [52]. A signal of about 2500 electrons is measured after a fluence of 10^{16} p/cm^2 and $8 \times 10^{15} \text{ n/cm}^2$.

On the basis of the above-mentioned experimental data simulations for a SLHC operation have been performed.

Fig. 7 demonstrates the development of the depletion voltage over a 5-year SLHC scenario for 25 and 50 μm thick epitaxial detectors which have been stored at two different temperatures (-7 and 20°C) during beam off periods. It is clearly visible that the detectors would profit

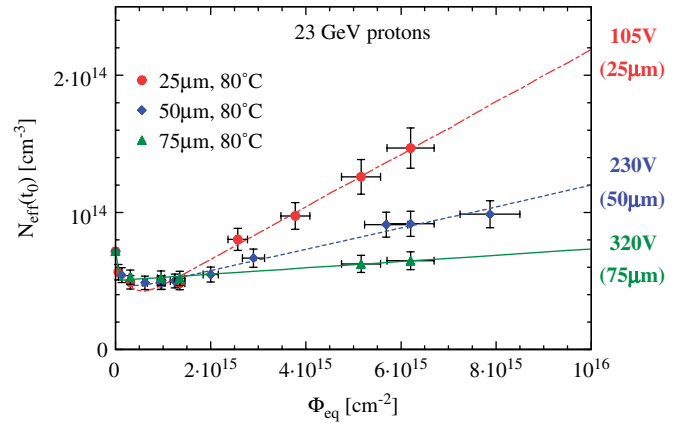


Fig. 5. Effective doping concentration measured after the end of the beneficial annealing as function of fluence for epitaxial silicon detectors of different thickness [48]. The values on the right-hand side indicate the depletion voltage expected for 10^{16} cm^{-2} .

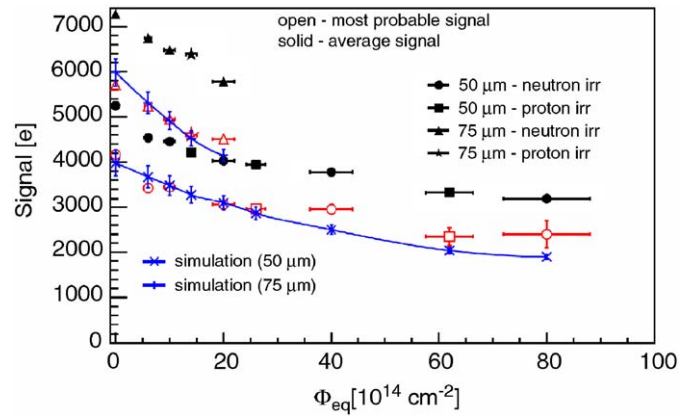


Fig. 6. Charge collected above full depletion for 50 and 75 μm thick epitaxial detectors. A fast read out electronics with 25 ns shaping has been used [52].

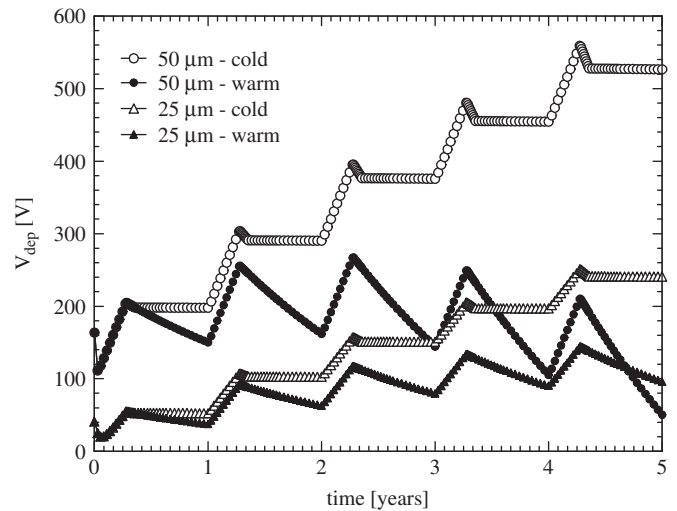


Fig. 7. Simulated depletion voltage for 25 and 50 μm epitaxial detectors during a 5-year SLHC operation. Every year the experiments are operated for 100 days at -7°C followed by a maintenance period of 30 days at 20°C . Finally the detectors are kept at -7°C in the “cold”-scenario and at 20°C for the “warm”-scenario for the rest of the year [48].

when they would not be cooled during beam off periods. The depletion voltage is decreasing due to the reverse annealing (the detectors are not type inverted) and at the same time the leakage current and the electron trapping decreases.

Fig. 8 shows another simulation based on data obtained within RD50. A pixel detector (in p^+n and n^+n technology) of an implant size of $50 \times 50 \mu\text{m}^2$ and a pitch of $70 \times 70 \mu\text{m}^2$ has been simulated in a “warm” SLHC scenario. The $75 \mu\text{m}$ thick epitaxial detectors type invert after about 1300 days. However, the main message is that about 2000 electrons would be delivered by a n^+n sensor at the end of the fifth year, which can be expected to be a pessimistic guess, since simulations tend to underestimate the delivered charge at high fluences (see Fig. 6 and Ref. [54]).

3.4. Silicon carbide and gallium nitride

The RD50 collaboration is investigating the use of SiC and GaN as alternative tracking detector material under special view of the SLHC project. The main characteristics of both materials are given in Table 1. Both materials offer a wider band gap than silicon which leads to a reduced leakage current and therefore allows for an operation at room temperature. However, the number of electron–hole pairs created per unit of radiation length is much less than in silicon. Extensive tests have now been performed in the framework of the RD50 project in order to understand if these materials offer a higher radiation tolerance than silicon. While on the one hand from the displacement threshold energy (see Table 1) a similar or even more tolerant behavior could be expected, on the other hand the fact that GaN and SiC are compound semiconductors could easily lead to a more radiation soft behavior due to the increased possibility of intrinsic defect creation.

4H–SiC has been tested in form of bulk ($\sim 100 \mu\text{m}$) and epitaxial ($\sim 7\text{--}50 \mu\text{m}$) material [7]. The bulk material was

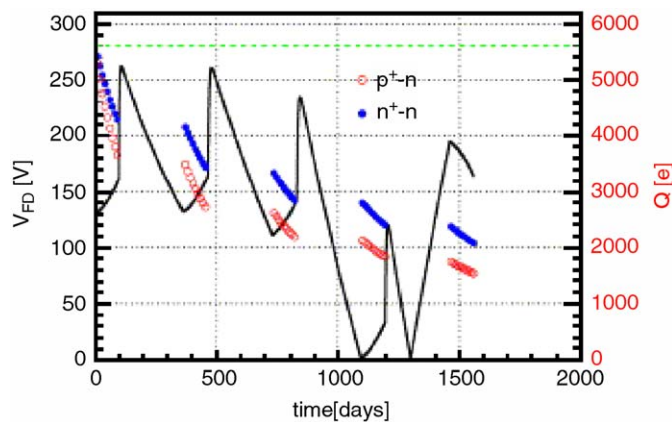


Fig. 8. Prediction of depletion voltage (solid line) and signal evolution (symbols) at SLHC for a $75 \mu\text{m}$ thick epitaxial detector. The assumed bias voltage was 280 V (dashed line).

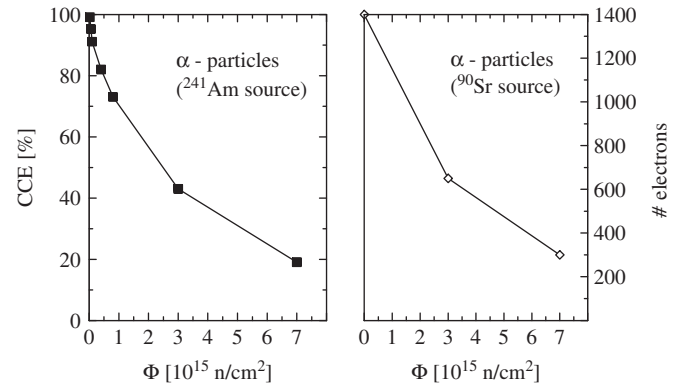


Fig. 9. Charge collection efficiency as function of neutron fluence as measured on 4H–SiC epitaxial diodes with a ^{241}Am -source (left) and a ^{90}Sr -source (right). Note that the β -particle measurement before irradiation was limited by a $25 \mu\text{m}$ depletion depth resulting from the low resistivity of the material. The measurements were performed with a low-noise readout system with a shaping time of $2 \mu\text{s}$ [57].

strongly Vanadium compensated in order to reach the high resistivity needed for particle detectors. Unfortunately the Vanadium led to the formation of defects before and even more after exposure to radiation that resulted in a strong reduction in CCE [55]. Only Vanadium-free bulk SiC therefore seems to be a feasible option. This is presently under investigation within RD50 [56].

Epitaxial 4H–SiC layers are meanwhile available in good quality. Schottky diodes made from 25 to $50 \mu\text{m}$ thick layers produced by CREE Research (USA) and IKZ (Berlin, Germany) have been proved to offer a 100% CCE as measured with β -particles from a ^{90}Sr -source [57]. However, after irradiation with protons and neutrons to fluences corresponding to those expected at the SLHC the material becomes intrinsic and the CCE is strongly reduced [57]. A measurement performed with α -particles after irradiation with different neutron fluences is shown in Fig. 9. After $7 \times 10^{15} \text{ n/cm}^2$ a CCE of only 20% was obtained at 600 V. Some measurements were performed with a ^{90}Sr -source. Before irradiation the material could be depleted to about $25 \mu\text{m}$ (200 V) giving a charge of 1400 ± 200 electrons. After $3 \times 10^{15} \text{ n/cm}^2$ the measured signal dropped to 650 electrons and after $7 \times 10^{15} \text{ n/cm}^2$ only 300 electrons were obtained (see Fig. 9). An irradiation with 23 GeV protons to $1.4 \times 10^{16} \text{ cm}^{-2}$ resulted in a signal of 370 electrons at 800 V. Presently irradiation tests of p^+n -diodes are under way to confirm these results [58].

Epitaxial GaN layers are presently only available in thin films of a few micrometers rendering a material characterization difficult. In a recent work diodes made from a $2.5 \mu\text{m}$ thick epitaxial GaN layer have been exposed to fast hadrons [56]. Measurements with an ^{241}Am -source showed that the CCE dropped from about 90% before irradiation to about 5% after an irradiation with 23 GeV protons to a fluence of 10^{16} cm^{-2} . Presently diodes made from $12 \mu\text{m}$ thick epitaxial GaN are under investigation within RD50 [59]. First results indicate that the unirradiated devices

have a CCE of 55% which is further reduced to 25% after an irradiation with 10^{16} p/cm².

4. Device engineering

4.1. Device engineering—overview

4.1.1. Reduction of drift length

After an irradiation with 10^{16} cm⁻² fast hadrons the effective drift length for charge carriers as well as the depletion depth for a given bias voltage are strongly reduced (see Section 2.1).

Several detector concepts have been proposed and developed to cope with this situation. In so-called “3D detectors” [60] the electrodes are an array of columns with $\sim 5\text{--}10\text{ }\mu\text{m}$ diameter placed at a distance of about $\sim 30\text{--}100\text{ }\mu\text{m}$ in a usually $300\text{ }\mu\text{m}$ thick wafer. The columns are filled alternately with p⁺- or n⁺-electrode material [60] (or are metallized to form Schottky contacts [61]). Since the electric field is evolving laterally from column to column, only $\sim 30\text{--}100\text{ }\mu\text{m}$ have to be depleted while the charge created by an ionizing particle is still that of a $300\text{ }\mu\text{m}$ thick detector. This technology is followed up by RD50 which however now is also focusing on a new simplified 3D concept presented in Section 4.2. Other concepts to reduce the depth that has to be depleted are Semi-3D detectors where alternatively p⁺ and n⁺ planar strip electrodes are placed on one or two detector surfaces [62] and the production of thin detectors. The latter are either produced from standard FZ wafers by chemical etching [63] or by using the “wafer-bonding” technology [64] and are coming along with a reduced radiation length or are grown as epitaxial layers on CZ silicon substrates (see Section 3.3).

4.1.2. Collection of electrons

In Section 2.1 it was pointed out that on the one hand electrons have a three times higher mobility than holes and on the other hand the annealing of the electron trapping is a beneficial effect, while the hole trapping becomes more detrimental. It is therefore important to collect electrons on the readout electrode which will be demonstrated in more detail in Section 4.3.

4.1.3. Reduction of detector costs

A low cost detector is always aimed for. However, the expected increase of granularity and the bigger surfaces to be covered with fine granularity tracking detectors in SLHC make a reduction in detector costs unavoidable to keep the project within an acceptable budget. The processing of the silicon detectors is compared to the material by far the major cost factor. This is also true for the defect engineered materials presented above. Therefore also the possibly lower costs of CZ silicon compared to FZ silicon has no significant influence on the detector price. A significant difference in costs is certainly the difference between single sided and double sided processing. Detectors based on n-in-p technology are less expensive than

detectors based on n-in-n technology. Single type column 3D detectors (STC-3D) detectors will be less expensive than 3D detectors. Further works in this direction are “Stripixels” [65] which are produced in a single sided double metal process and should give a track resolution equivalent to a double sided strip detector or even a pixel detector with a yet reduced cost.

4.2. Single type column 3D detectors

A drawback of 3D detectors is their rather complicated fabrication process. Recently a single type column 3D detector has been proposed [66]. It offers a significant simplification of the production process since the column etching and doping is performed only once. Fig. 10 shows a sketch of a STC-3D with n⁺ electrodes in a p-type bulk.

One of the major concerns with respect to 3D devices with two types of columns are the zero-field regions in the center of four columns where the charge carriers move only by diffusion. However, simulations with the ATLAS package by Silvaco (see Fig. 11) give confidence that even for particles traversing the zero-field region the charge can be collected within 10 ns. Fabrication of first devices has very recently been completed at IRST in Trento, Italy. Preliminary results from electrical characterization demonstrate the feasibility of the technological approach [67].

4.3. Detectors on p-type silicon

Sensors with a structured n⁺ implant on n-type silicon, so-called n-in-n sensors, are used for pixel and micro-strip detectors that have to operate in extreme radiation fields. Present examples are the ATLAS and CMS pixel detectors [68,69] and the LHCb VELO detector [70]. The advantage of the n-in-n configuration is found after high irradiation levels. When the bulk of the sensor has undergone type inversion the high electric field will be on the structured n⁺ electrode and thus assure significant charge collection even if operated with a voltage below full depletion. Contrary,

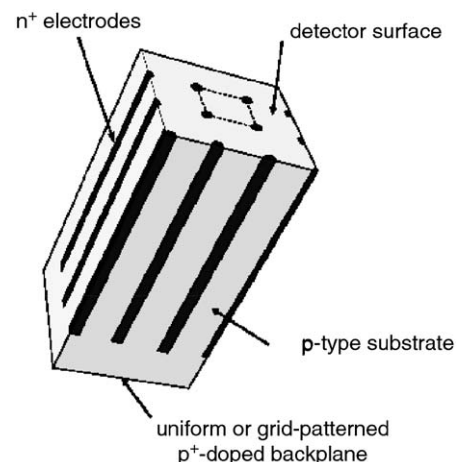


Fig. 10. Sketch of a 3D detector featuring columnar electrodes of one doping type [66].

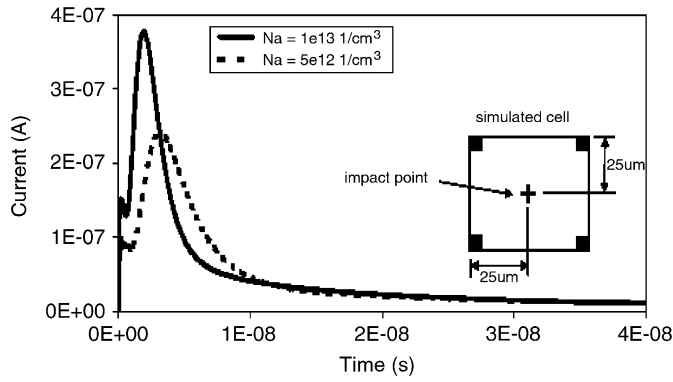


Fig. 11. Simulation of the current induced by a particle impinging at the center of four electrode columns (zero-field region) for two p-type STC-3D detectors with different doping concentrations as indicated in the legend [66].

for highly irradiated standard p-in-n detectors the high electric field would be on the non-structured n^+ back electrode thus requiring a high voltage applied to the detector to assure a sufficiently strong electric field at the structured side of the detector. Furthermore, electrons are collected at the segmented electrode in n-in-n detectors. Since they have a three times higher mobility than holes, trapping is reduced for the carriers collected at the structured electrode contributing to a more efficient charge collection.

However, a price has to be paid. The n-in-n sensors have to be produced in double-sided processing and before type inversion of the bulk the sensors have to be operated in an over biased way since the high electric field is on the non-structured side of the detector. Taking into account the advantages of the n-in-n technology, the question arises why not to use directly n-in-p devices. The high electric field will be at the structured electrode before and after irradiation since the bulk material is of p-type already before irradiation and thus does not invert, electrons will be collected at the structured electrode and only single-sided processing will be required.

As for the n-in-p processing care has to be taken for the n-in-p strip or pixel isolation. Since positive charge is accumulating in the SiO_2 and the SiO_2 -Si interface by ionizing irradiation a conductive channel can be formed between the n-electrodes leading to shorts between them. To cope with this either p-type channels (p-stops) or a moderate p implantation over the full surface (p-spray) has to be done. Both techniques are presently under investigation for p-type particle detectors in the framework of the RD50 project. No significant problems were encountered so far in dealing with this technology.

First measurements on ministrip detectors irradiated with 23 GeV protons up to $3 \times 10^{14} \text{ cm}^{-2}$ showed that p-type detectors give a higher signal at depletion than standard n-type detectors and a significantly higher signal if the detector is operated slightly underdepleted [71]. Later on experiments on oxygenated and standard p-type

microstrip detectors were performed up to a 23 GeV proton fluence of $7.5 \times 10^{15} \text{ cm}^{-2}$ [72]. The charge collected for the $1 \times 1 \text{ cm}^2$ and 280 μm thick p-type microstrip detectors as function of fluence is shown in Fig. 12. Even after a fluence of $7.5 \times 10^{15} \text{ cm}^{-2}$ about 6500 electrons are collected resulting in a signal over noise value of ~ 7.5 which is still a reasonable value for tracking.

An even more encouraging result was recently obtained during an accelerated annealing test at 80 °C performed to

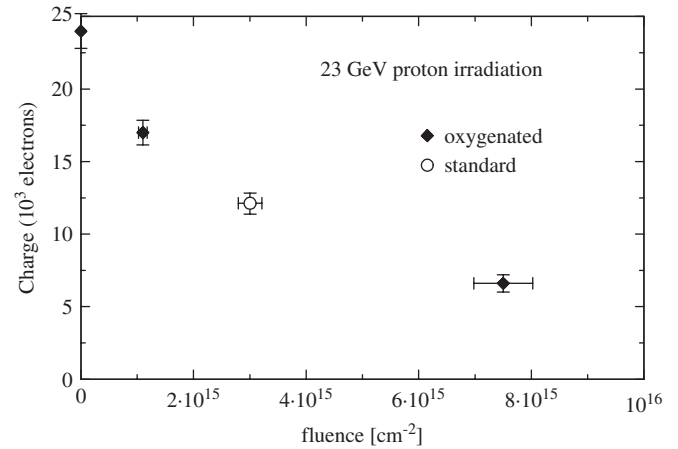


Fig. 12. Collected charge as a function of the 23 GeV proton fluence for standard and oxygenated n-in-p miniature microstrip detectors (source: Ru106, chip: SCT128A–40 MHz, 800–900 V applied to irradiated devices, measured at -20°C) [72].

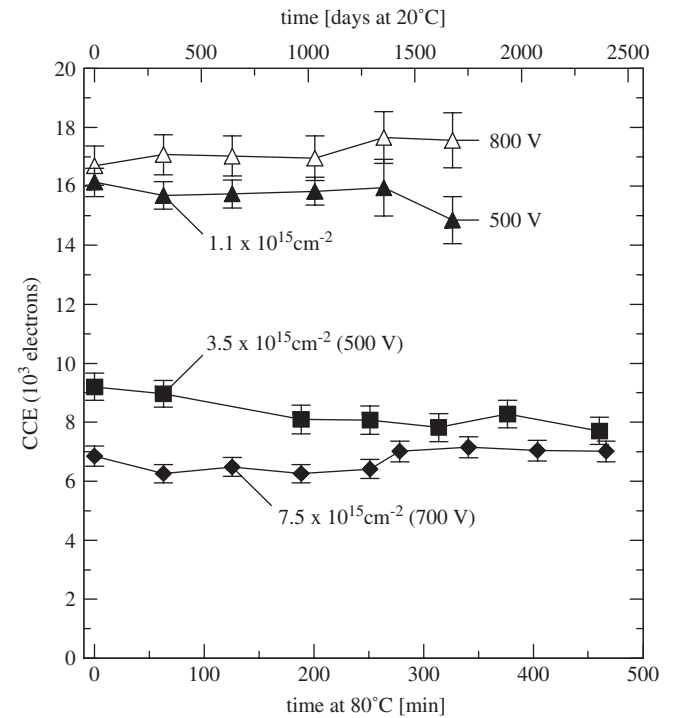


Fig. 13. Collected charge as function of annealing time at 80 °C. The same devices as presented in Fig. 12 have been used. The 23 GeV proton fluence and the voltage applied to the detector are indicated [73]. The upper timescale shows the equivalent time at room temperature using a scaling factor given in Ref. [76] for the reverse annealing.

investigate on reverse annealing effects of the CCE [73]. As demonstrated in Fig. 13 the CCE is not following the trend of the effective doping concentration but stays constant.

This is a very positive result and a clear demonstration that it is not straightforward to predict the CCE from the detector depletion voltage. In the particular case of the detector irradiated with 10^{15} cm^{-2} a depletion voltage of 2.8 kV would be expected after irradiation which should rise during the reverse annealing to about 12 kV [73]. However, almost no decrease in the CCE is observed. This is indicating that besides the change of the effective doping concentration the particular detector geometry and the fact that the effective electron trapping time is increasing by about 20–50% during the reverse annealing [18,74] play a major role for the evolution of the CCE. A complex behavior that can only be modeled and understood with comprehensive simulation tools (see e.g. Ref. [75]).

5. Conclusion

A review of research activities related to the development of radiation tolerant sensors for the Super-LHC project has been given including several detailed examples of the work performed by the RD50 collaboration.

CZ and epitaxial n-type silicon were shown to be more radiation tolerant than standard FZ silicon with respect to the change of the effective doping concentration. The fact that both materials do not undergo space charge sign inversion can be exploited to produce cost-effective and radiation tolerant p-in-n detectors. They would not even need to be cooled when not operated, since they, unlike standard FZ detectors, would profit from the reverse annealing effect. While CZ silicon could thus well become a cost-effective option for strip detectors in the outer tracking regions of SLHC experiments, EPI could be an option for the pixel detectors. Measurements demonstrate that about 2500 electrons can be collected with 50 μm thick epitaxial layers after the highest expected SLHC fluence (10^{16} cm^{-2}).

Investigations on SiC and GaN detectors showed that these materials are susceptible to radiation damage and seem not to offer an alternative to silicon in the near future.

Studies on p-type silicon ministrip detectors revealed an unexpected high charge yield (6500 electrons after an irradiation to $7.5 \times 10^{15} \text{ p/cm}^2$) making them a very promising choice for SLHC outer tracking layers. The recent result that the charge yield after high radiation levels is not affected by the reverse annealing makes this approach even more promising. However, this experiment demonstrated also very clearly that not only the choice of material but also the device structure has a very strong impact on the radiation tolerance and that predictions valid for one type of structure (simple pad) to more complex structures (strip, pixel) are not straightforward.

Finally, latest approaches to produce 3D detectors have been presented. If the technological difficulties can be overcome and tests of the prototypes are positive, they will

become “the solution” for the innermost pixel layers in the SLHC experiments.

References

- [1] LHC Project Report 626, F. Ruggiero (Ed.), LHC Luminosity and Energy Upgrade: A Feasibility Study, CERN, December 2002, <http://cern.ch/lhc-proj-IR-upgrade/>.
- [2] F. Gianotti, et al., Physics potential and experimental challenges of the LHC luminosity upgrade, hep-ph/0204087, April 2002.
- [3] G. Lindström, Nucl. Instr. and Meth. A 512 (2003) 30.
- [4] The RD50 collaboration; <http://cern.ch/rd50/>.
- [5] ATLAS Tracker Upgrade Workshop, Genova, July 18–20, 2005, Physics Department of University & INFN and previous upgrade workshops.
- [6] 3rd CMS Workshop on Detectors and Electronics for SLHC, CERN, Geneva, Switzerland July 15–16, 2005 and previous upgrade workshops.
- [7] RD50 Status Report 2004; CERN-LHCC-2004-031, LHCC-RD-005 (available on Ref. [4]).
- [8] E. Fretwurst, et al., Nucl. Instr. and Meth. A 552 (2005) 7.
- [9] M. Moll, et al., Nucl. Instr. and Meth. A 546 (2005) 99.
- [10] M. Bruzzi, et al., Nucl. Instr. and Meth. A 541 (2005) 189.
- [11] M. Moll, Nucl. Instr. and Meth. A 511 (2003) 97.
- [12] M. Moll, E. Fretwurst, M. Kuhnke, G. Lindström, Nucl. Instr. and Meth. B 186 (2002) 100.
- [13] G. Kramberger, V. Cindro, I. Mandić, M. Mikuž, M. Zavrtanik, Nucl. Instr. and Meth. A 476 (2002) 645.
- [14] A.G. Bates, M. Moll, Nucl. Instr. and Meth. A 555 (2005) 113.
- [15] RD48, “3rd Status Report”, CERN/LHCC 2000-009, December 1999.
- [16] V. Eremin, E. Verbitskaya, Z. Li, Nucl. Instr. and Meth. A 476 (2002) 556.
- [17] M. Swartz, et al., Observation, modeling, and temperature dependence of doubly peaked electric fields in irradiated silicon pixel sensors, Nucl. Instr. and Meth. A, these proceedings, doi:10.1016/j.nima.2006.05.002.
- [18] G. Kramberger, V. Cindro, I. Mandić, M. Mikuž, M. Zavrtanik, Nucl. Instr. and Meth. A 481 (2002) 297.
- [19] G. Lindström, et al., Nucl. Instr. and Meth. A 466 (2001) 308.
- [20] G. Lindstroem, E. Fretwurst, G. Kramberger, I. Pintilie, J. Optoelectron. Adv. Mater. 6 (1) (2004) 23.
- [21] Z. Li, Ultra-hard sensors for particle physics applications, in: Proceedings of the Pixel 2002 International Workshop, Carmel, CA, USA, 2002 (eConf C020909 (2002)).
- [22] J. Wüstenfeld, Characterisation of ionisation-induced surface effects for the optimisation of silicon-detectors for particle physics applications, Ph.D. Thesis, University of Dortmund, August 2001.
- [23] I. Pintilie, E. Fretwurst, G. Lindström, J. Stahl, Nucl. Instr. and Meth. A 514 (2003) 18.
- [24] The RD39 Collaboration, Cryogenic tracking detectors, <http://www.cern.ch/rd39>.
- [25] RD48, 2nd Status Report, CERN LHCC 98-39, LEB Status Report/RD48, 21 October 1998.
- [26] O. Lytovchenko, Radiation hardness of silicon detectors based on preirradiated silicon, Presented on the 10th European Symposium on Semiconductor Detectors, Wildbad Kreuth, June 12–16, 2005, Nucl. Instr. and Meth. A, to be published.
- [27] V. Boisvert, J.L. Lindström, M. Moll, L.I. Murin, I. Pintilie, Nucl. Instr. and Meth. A 552 (2005) 49.
- [28] L.F. Makarenko, F.P. Korshunov, S.B. Lastovski, N.M. Kazuchits, M.S. Rusetsky, E. Fretwurst, G. Lindström, M. Moll, I. Pintilie, N.I. Zamiatin, Nucl. Instr. and Meth. A 552 (2005) 77.
- [29] RD42 Collaboration, CVD diamond radiation detector development, <http://www.cern.ch/rd42>.
- [30] H. Kagan, Nucl. Instr. and Meth. A 546 (2005) 222.

- [31] N. Wyrsh, S. Dunand, C. Miazza, A. Shah, G. Anelli, M. Despeisse, A. Garrigos, P. Jarron, J. Kaplon, D. Moraes, S.C. Commichau, G. Dissertori, G.M. Viertel, *Phys. Stat. Sol. (c)* 1 (5) (2004) 1284.
- [32] P.J. Sellin, J. Vaitkus, on behalf of RD50, *Nucl. Instr. and Meth. A* 557 (2006) 479–489.
- [33] S.M. Sze, *Semiconductor Devices—Physics and Technology*, second ed, Wiley, New York, 1985, 2002.
- [34] S. Eidelman, et al., *Phys. Lett. B* 592 (2004) 1.
- [35] G. Lutz, *Semiconductor Radiation Detectors*, Springer, Berlin, 1999.
- [36] M. Rogalla, K. Runge, A. Söldner-Rembold, *Nucl. Phys. B (Proc. Suppl.)* 78 (1999) 516.
- [37] F. Moscatelli, A. Scorzoni, A. Poggi, M. Bruzzi, S. Lagomarsino, S. Mersi, S. Sciortino, R. Nipoti, *Nucl. Instr. and Meth. A* 546 (2005) 218.
- [38] M. Rogalla, Systematic investigation of gallium arsenide radiation detectors for high energy physics experiments, Ph.D. Thesis, University of Freiburg, December 1997.
- [39] Landolt-Börnstein, New Series III/22a, Intrinsic Properties of Group IV Elements and II–V, II–VI and I–VII Compounds, Springer, Berlin, 1987.
- [40] G.C. Messenger, M.S. Ash, *The Effects of Radiation on Electronic Systems*, second ed, Van Nostrand Reinhold, New York, 1992.
- [41] R. Aleksan, T. Bolgnesi, B. Equer, A. Karar, J.M. Reymond, *Nucl. Instr. and Meth. A* 305 (1991) 512.
- [42] A. Barcz, M. Zielinski, E. Nossarzewska, G. Lindström, *Appl. Surf. Sci.* 203–204 (2003) 396.
- [43] Z. Li, M. Bruzzi, V. Eremin, J. Harkonen, J. Kierstead, P. Luukka, D. Menichelli, Tuominen, E. Tuovinen, E. Verbitskaya, *Nucl. Instr. and Meth. A* 552 (2005) 34.
- [44] G. Pellegrini, M. Ullán, J.M. Rafí, C. Fleta, F. Campabadal, M. Lozano, *Nucl. Instr. and Meth. A* 552 (2005) 27.
- [45] J. Härkönen, et al., *Nucl. Instr. and Meth. A* 518 (2004) 346.
- [46] E. Fretwurst, et al., Survey of recent radiation damage studies at Hamburg, presented on the Third RD50 Workshop, 3–5 November 2003, CERN, Geneva, Switzerland (see Ref. [4]).
- [47] S. Dittongo, L. Bosisio, D. Contarato, G. D’Auria, E. Fretwurst, J. Härkönen, G. Lindström, E. Tuovinen, *Nucl. Instr. and Meth. A* 546 (2005) 300.
- [48] G. Lindström, I. Dolenc, E. Fretwurst, F. Hönniger, G. Kramberger, M. Moll, E. Nossarzewska, I. Pintilie, R. Röder, Epitaxial silicon detectors for particle tracking-radiation tolerance at extreme hadron fluences, presented on the 10th European Symposium on Semiconductor Detectors, Wildbad Kreuth, June 12–16, 2005, *Nucl. Instr. and Meth. A*, to be published.
- [49] I. Pintilie, M. Buda, E. Fretwurst, G. Lindström, J. Stahl, Stable radiation induced donor generation and its influence on the radiation tolerance of silicon diodes, *Nucl. Instr. and Meth. A*, submitted for publication.
- [50] B. Dezillie, F. Lemeilleur, M. Glaser, G.-L. Casse, C. Lerory, *Nucl. Instr. and Meth. A* 386 (1997) 162.
- [51] G. Kramberger, D. Contarato, E. Fretwurst, F. Hönniger, G. Lindström, I. Pintilie, R. Röder, A. Schramm, J. Stahl, *Nucl. Instr. and Meth. A* 515 (2003) 665.
- [52] G. Kramberger, V. Cindro, I. Dolenc, E. Fretwurst, G. Lindström, I. Mandić, M. Mikuž, M. Zavrtanik, *Nucl. Instr. and Meth. A* 554 (2005) 212–219.
- [53] A. Candelori, A. Schramm, D. Bisello, D. Contarato, E. Fretwurst, G. Lindström, R. Rando, J. Wyss, *IEEE Trans. Nucl. Sci. NS-51* (2004) 1766.
- [54] T. Lari, *Nucl. Instr. and Meth. A* 560 (2006) 93.
- [55] W. Cunningham, J. Melone, M. Horn, V. Kazukauskas, P. Roy, F. Doherty, M. Glaser, J. Vaitkus, M. Rahman, *Nucl. Instr. and Meth. A* 509 (2003) 127.
- [56] J. Grant, W. Cunningham, A. Blue, V. O’Shea, J. Vaitkus, E. Gaubas, M. Rahman, *Nucl. Instr. and Meth. A* 546 (2005) 213.
- [57] S. Sciortino, F. Hartjes, S. Lagomarsino, F. Nava, M. Brianzi, V. Cindro, C. Lanzieri, M. Moll, P. Vanni, *Nucl. Instr. and Meth. A* 552 (2005) 138.
- [58] F. Moscatelli, A. Scorzoni, A. Poggi, M. Bruzzi, S. Lagomarsino, S. Mersi, S. Sciortino, R. Nipoti, *Nucl. Instr. and Meth. A* 546 (2005) 218.
- [59] J. Grant, R. Bates, A. Blue, W. Cunningham, J. Vaitkus, E. Gaubas, V.O.’Shea, I–V & CCE Characterisation of proton irradiated 12 micron epitaxial GaN detectors, presented on the Sixth RD50 Workshop, Helsinki, Finland, 2–4 June, 2005 (see Ref. [4]).
- [60] S.I. Parker, C.J. Kenney, J. Segal, *Nucl. Instr. and Meth. A* 395 (1997) 328.
- [61] G. Pellegrini, et al., *Nucl. Instr. and Meth. A* 487 (2002) 19.
- [62] Z. Li, R. Beuttenmuller, W. Chen, D. Elliott, V. Radeka, J. Takahashi, W.C. Zhang, *Nucl. Instr. and Meth. A* 478 (2002) 303.
- [63] S. Ronchin, M. Boscardin, G.-F. Dalla Betta, P. Gregori, V. Guarnieri, C. Piemonte, N. Zorzi, *Nucl. Instr. and Meth. A* 530 (2004) 134.
- [64] L. Andricek, G. Lutz, M. Reiche, R.H. Richter, *IEEE Trans. Nucl. Sci. NS-51* (3) (2004) 1117.
- [65] Z. Li, *Nucl. Instr. and Meth. A* 518 (2004) 738.
- [66] C. Piemonte, M. Boscardin, G.-F. Dalla Betta, S. Ronchin, N. Zorzi, *Nucl. Instr. and Meth. A* 541 (2005) 441.
- [67] S. Ronchin, M. Boscardin, C. Piemonte, A. Pozza, N. Zorzia, G.-F. Dalla Betta, L. Bosisio, G. Pellegrini, Fabrication of 3D detectors with columnar electrodes of the same doping type, presented on the Seventh International Conference on Position Sensitive Detectors, Liverpool, September 12–16, 2005, *Nucl. Instr. and Meth. A*, submitted for publication.
- [68] G. Gagliardi, *Nucl. Instr. and Meth. A* 546 (2005) 67 (see also ATLAS Pixel Detector TDR, CERN/LHCC/98-13, ATLAS TDR 11, 31 May 1998).
- [69] A. Dorokhov, et al., *Nucl. Instr. and Meth. A* 530 (2004) 71 (see also CMS Tracker Technical Design Report, CERN/LHCC/98-6, 15 April 1998).
- [70] L. Eklund, *Nucl. Instr. and Meth. A* 546 (2005) 72 (see also LHCb VELO TDR, CERN/LHCC 2001-0011, LHCb TDR 5, 31 May 2001).
- [71] G. Casse, P.P. Allport, T.J.V. Bowcock, A. Greenall, M. Hanlon, J.N. Jackson, *Nucl. Instr. and Meth. A* 487 (2002) 465.
- [72] G. Casse, P.P. Allport, S. Martí i Garcia, M. Lozano, P.R. Turner, *Nucl. Instr. and Meth. A* 535 (2004) 362.
- [73] G. Casse, P.P. Allport, A. Watson, Effects of accelerated annealing on p-type silicon micro-strip detectors after very high doses of proton irradiation, Paper presented on the 10th European Symposium on Semiconductor Detectors, 12–16 June 2005, Wildbad Kreuth, Germany, *Nucl. Instr. and Meth. A*, to be published.
- [74] O. Krasel, Charge collection in irradiated silicon-detectors, Ph.D. Thesis, University of Dortmund, July 2004.
- [75] M. Petasecca, F. Moscatelli, D. Passeri, G. Pignatelli, A comprehensive numerical simulation of heavily irradiated p-type silicon detectors, Presented on the IEEE Nuclear Science Symposium 2005, October 23–29, Puerto Rico, IEEE Nucl. Sci., to be published.
- [76] M. Moll, Radiation damage in silicon particle detectors—microscopic defects and macroscopic properties, Ph.D. Thesis, DESY-THESIS-1999-040, University of Hamburg, December 1999.